

Localization-Delocalization quantum Hall transition in the presence of a quenched disorder

P. Cain, R. A. Römer, and M. Schreiber

Institut für Physik, Technische Universität Chemnitz, D-09107 Chemnitz, Germany

M. E. Raikh

Department of Physics, University of Utah, Salt Lake City, UT 84112, U.S.A.

(Revision : 1.35, compiled February 7, 2020)

We study theoretically the effect of long-ranged inhomogeneities on the critical properties of the integer quantum Hall transition. For this purpose we employ the real-space renormalization-group (RG) approach to the network model of the transition. We start with testing the accuracy of the RG approach in the absence of inhomogeneities and infer the correlation length exponent $\nu = 2.39$ from a broad conductance distribution. We then incorporate macroscopic inhomogeneities into the RG procedure. Inhomogeneities are modeled by a smooth random potential with a correlator which falls off with distance as a *power law*, $r^{-\alpha}$. Similar to the classical percolation, we observe the enhancement of ν with decreasing α . Although the attainable system sizes are big, they do not allow to identify a cusp in the $\nu(\alpha)$ dependence at $\alpha_c = 2/\nu$, as might be expected from the extended Harris criterion. We argue that the underlying reason for the absence of the cusp in the *quantum* percolation is the implicit randomness in the *Aharonov-Bohm phases* of the wave functions. This randomness emulates the presence of a *short-range* disorder alongside with the smooth potential.

PACS numbers: 73.40.Hm, 61.43.-j, 64.60.Ak

I. INTRODUCTION

The critical behavior of electron wave functions in the vicinity of the integer quantum Hall (QH) transition is now well understood [1]. Namely, the localization length diverges as $\varepsilon^{-\nu}$, where ε is the deviation from the critical energy. The most accurate value of the exponent ν extracted from numerical simulations is $\nu = 2.35 \pm 0.03$ [2]. On the experimental side, the study of the critical behavior of the resistance in the transition region at strong magnetic field B has a long history which can be conventionally divided into three periods.

a. The first experimental works [3–9] reported the narrowing of the transition peak with temperature, T , as T^κ with $\kappa \sim 0.4$. The spread in the actual value of $\kappa \propto 1/\nu$ measured in different experiments has been attributed to the difference in the type of disorder in the samples of Refs. [3,4] and [5]. Another experimental method to explore the critical behavior was employed in Refs. [6,7], where κ was deduced from the sample size dependence of the width, ΔB , of the transition region. The value of κ obtained by this technique appeared to be consistent with temperature measurements of Ref. [5], in the sense that κ was found to be sample dependent. On the other hand, it was argued in Ref. [8] that the lack of universality in Refs. [5–7] has its origin in the long-ranged character of the disorder in GaAs-based heterostructures studied in these works. This is because for a smooth disorder the energy interval within which the electron transport is dominated by localization effects is relatively narrow [8]. The measurements in Refs. [3,4] suggesting the universality of κ were carried out on InGaAs/InP heterostructures in which disorder is believed to be short-ranged [10]. Despite the disagreement about universality

of the exponent κ , the fact that the narrowing of the plateau transition occurs as T^κ was not questioned in Refs. [3–9].

b. Absence of scaling was reported first for the QH-insulator [11] and then for the plateau-plateau transition [12]. In the latter paper the conclusion about the absence of scaling was drawn from the analysis of the frequency dependence of ΔB in GaAs/AlGaAs heterostructures (in contrast to the similar analysis in Ref. [13]). Namely, the authors of Refs. [11,12] conclude that the width of the transition region *saturates* as $T \rightarrow 0$. A possible explanation of this behavior [14,15] is based on the scenario of tunneling between electron puddles with a size larger than the dephasing length. The microscopic origin of these puddles was attributed to sample inhomogeneities [16–18].

c. Very recent experimental results [19] on scaling of plateau-insulator as well as plateau-plateau QH transitions carried out on the same InGaAs/InP sample as in Ref. [9] suggest that the narrowing of the transition width with temperature follows the power-law dependence $\Delta B \propto T^\kappa$ with $\kappa \approx 0.4$. Even when the authors of Ref. [19] analyzed their data using the procedure of Ref. [11], i.e., by plotting the logarithm of the longitudinal resistance versus ΔB , they obtained straight lines with slopes proportional to $T^{\kappa'}$ with $\kappa' \approx 0.55$. They attributed the difference between κ and κ' to the marginal dependence of the critical resistance on T . It is also speculated in Ref. [19] that this dependence most likely results from macroscopic inhomogeneities in the sample. In the latest papers [20–22] the frequency dependence of the QH transition width was studied. The results do not support the saturation of the width [11,12], but rather confirm the scaling hypothesis.

Summarizing, it is now conclusively established that insulator-plateau and plateau-plateau transitions exhibit the same critical behavior. It is also recognized that macroscopic inhomogeneities can either mask the scaling or alter the value of κ [19].

On the theoretical side, in all previous considerations inhomogeneities were incorporated into the theory through the spatial variation of the *local* resistivity [14–18,23]. In other words, all existing theories are either "homogeneous quantum coherent" or "inhomogeneous incoherent". Meanwhile, there is another scenario which has never been explored. Close to the transition the *quantum* localization length ξ becomes sufficiently large. Then the long-ranged disorder can affect the character of the divergence of ξ . At this point we recall the classical limit [24,25] in which the long-ranged disorder does affect the value of the critical exponent in the percolation problem. Obviously, when the disorder is long-ranged but has a finite correlation radius one should not expect any changes in the critical behavior. The principle finding of Refs. [24,25] is that the critical exponent can change when the correlator of the disorder $\langle V(\mathbf{r})V(\mathbf{r}') \rangle$ falls off with distance as a power law, i.e., $\propto |\mathbf{r}-\mathbf{r}'|^{-\alpha}$, (quenched disorder). According to Refs. [24,25] the critical exponent of the classical percolation $\nu = 4/3$ crosses over to $\nu = 2/\alpha$ for $\alpha < 3/2$, i.e., when the decay of the correlator is slow enough. In the present paper we study the effects of quenched disorder on *quantum* percolation. The latter is known to describe the localization-delocalization transition for a two-dimensional (2D) electron in a strong magnetic field. As a model of quantum percolation we employ the Chalker-Coddington (CC) model [26] which is one of the main "tools" for the quantitative study of the QH transition [27–38]. The CC model is a strong magnetic field (chiral) limit of a general network model, first introduced by Shapiro [39] and later utilized for the study of localization-delocalization transitions within different universality classes [40–45]. In addition to describing the QH transition the CC model applies to a much broader class of critical phenomena since the correspondence between the CC model and thermodynamic, field-theory and Dirac-fermions models [46–54] was demonstrated.

In order to study the role of the quenched disorder on the localization-delocalization transition we treat the CC model within the real-space renormalization group (RG) approach. First we check in Sec. II the accuracy of the RG approach and show that it provides a remarkably accurate description of the QH transition. In Sec. III we extend the RG approach to incorporate the quenched disorder. Concluding remarks are presented in Sec. IV.

II. TEST OF THE RG APPROACH TO THE CC MODEL

A. Description of the RG approach

As it was mentioned in the Introduction, the CC model is a chiral limit of the general network model [39]. However, it was originally derived from the microscopic picture of electron motion in a strong magnetic field and a smooth potential [26]. Within this picture, the links can be identified with semiclassical trajectories of the guiding centers of the cyclotron orbit, while the nodes correspond to the saddle points (SPs) at which different trajectories come closer than the Larmor radius. For simplicity, the nodes were placed on a square lattice. We will use an equivalent, but slightly different graphical representation of the CC network shown in Fig. 1. In this representation the centers of the trajectories of the guiding centers are placed on a square lattice and play the role of nodes, whereas the SPs should be identified with links.

We now apply a real-space RG [55,56] to the CC network [57,58]. The RG approach is based on the assumption that a certain part of the network containing several SPs, the RG unit, represents the entire network. This unit is then replaced through the RG transformation by a single *super*-SP with an *S*-matrix determined by the *S*-matrices of the constituting SPs. The network of super-SPs is then treated in the same way as the original network. Successive repetition of the RG transformation yields the information about the *S*-matrix of very large samples, since after each RG step, the effective sample size grows by a certain factor determined by the geometry of the original RG unit. Obviously, a single RG unit is a rather crude approximation of the network. Therefore, prior to applying the RG approach to the study of the quantum Hall transition in the presence of the quenched disorder, we first check the accuracy of this approach for the conventional, uncorrelated case, where the comparison with the results of direct numerical simulations is possible.

The RG unit we use is extracted from a CC network on a regular 2D square lattice as shown in Fig. 1. A super-SP consists of 5 original SPs by analogy to the RG unit employed for the 2D bond percolation problem [59–61]. Between the SPs an electron travels along equipotential lines and accumulates a certain Aharonov-Bohm phase. Different phases are uncorrelated, which reflects the randomness of the original potential landscape. Each SP can be described by two equations relating the wave function amplitudes in incoming and outgoing channels. This results in a system of 10 linear equations, the solution of which yields the following expression for the transmission coefficient of the super-SP [55]

$$t' = \left| \frac{t_1 t_5 (r_2 r_3 r_4 e^{i\Phi_2} - 1) + t_2 t_4 e^{i(\Phi_3 + \Phi_4)} (r_1 r_3 r_5 e^{-i\Phi_1} - 1) + t_3 (t_2 t_5 e^{i\Phi_3} + t_1 t_4 e^{i\Phi_4})}{(r_3 - r_2 r_4 e^{i\Phi_2})(r_3 - r_1 r_5 e^{i\Phi_1}) + (t_3 - t_4 t_5 e^{i\Phi_4})(t_3 - t_1 t_2 e^{i\Phi_3})} \right|. \quad (1)$$

Here t_i and $r_i = (1 - t_i^2)^{1/2}$ are, respectively, the transmission and reflection coefficients of the constituting SPs; Φ_j are the phases accumulated along the closed loops (see Fig. 1). Eq. (1) is the RG transformation, which allows to generate (after averaging over Φ_j) the distribution $P(t')$ of the transmission coefficients of super-SPs using the distribution $P(t)$ of the transmission coefficients of the original SPs. Since the transmission coefficients of the original SPs depend on the electron energy, ε , the fact that delocalization occurs at $\varepsilon = 0$ implies that a certain distribution, $P_c(t)$ — with $P_c(t^2)$ being symmetric with respect to $t^2 = \frac{1}{2}$ — is the fixed point (FP) of the RG transformation Eq. (1). The distribution $P_c(G)$ of the dimensionless conductance, G , can be obtained from the relation $G = t^2$, so that $P_c(G) \equiv P_c(t)/2t$.

B. Critical exponent within the RG approach

Since the dimensionless SP height z_i and the transmission coefficient t_i at $\varepsilon = 0$ are related as $t_i = (e^{z_i} + 1)^{-1/2}$, the transformation (1) determines the height of a super-SP through the heights of the 5 constituting SPs. Correspondingly, the distribution $P(G)$ determines the distribution $Q(z)$ of the SP heights $Q(z) = \frac{1}{4} \cosh^{-2}(z/2) P[(e^z + 1)^{-1}]$. The language of the SP heights provides a natural way to extract the critical exponent ν . Suppose that the RG procedure starts with an initial distribution, $Q_0(z) = Q_c(z - z_0)$, that is shifted from the critical distribution, $Q_c(z)$, by a small $z_0 \propto \varepsilon$. Since $z_0 \ll 1$ the first RG step would yield $Q_c(z - \tau z_0)$ with some number τ independent of z_0 . After n steps the center of the distribution will get shifted by $z_{\max, n} = \tau^n z_0$, while the sample size will get magnified by 2^n . At the n -th step corresponding to $z_{\max, n} \sim 1$ a typical SP is not transmittable anymore. Then the localization length ξ should be identified with $2^n \propto z_0^{-\nu} \propto \varepsilon^{-\nu}$, with $\nu = \ln 2 / \ln \tau$. When the RG procedure is carried out numerically, one should check that z_0 is small enough, so that $z_{\max, n} \propto z_0$ for large enough n . Consequently, the working formula for the critical exponent can be presented as

$$\nu = \frac{\ln 2^n}{\ln \left(\frac{z_{\max, n}}{z_0} \right)} \quad (2)$$

which should be independent of n for large n .

C. Numerical results

In order to find the FP conductance distribution $P_c(G)$ we start from a certain initial distribution of transmission coefficients, $P_0(t)$ (see below). The distribution is

discretized in at least 1000 bins such that the bin width is typically 0.001 for the interval $t \in [0, 1]$. From $P_0(t)$, we obtain t_i , $i = 1, \dots, 5$ and substitute them into the RG transformation (1). The phases Φ_j , $j = 1, \dots, 4$ are chosen randomly from the interval $\Phi_j \in [0, 2\pi]$. In this way we calculate at least 10^7 super-transmission coefficients t' . The obtained histogram, $P_1(t')$, is then smoothed using a Savitzky-Golay filter [62] in order to decrease statistical fluctuations. At the next step we repeat the procedure using P_1 as an initial distribution. We assume that the iteration process has converged when the mean square deviation $\int dt [P_n(t) - P_{n-1}(t)]^2$ of the distribution P_n and its predecessor P_{n-1} deviate by less than 10^{-4} .

We are now able to study the samples with short-ranged disorder. The actual initial distributions, $P_0(t)$, were chosen in such a way that corresponding conductance distributions, $P_0(G)$, were either uniform or parabolic, or identical to the FP distribution found semi-analytically in Ref. [55]. All these distributions are symmetric with respect to $G = 0.5$. We find that, regardless of the choice of the initial distribution, after 5–10 steps the RG procedure converges to the *same* FP distribution which remains unchanged for another 4–6 RG steps. Small deviations from symmetry about $G = 0.5$ finally accumulate due to numerical instabilities in the RG procedure, so that typically after 15–20 iterations the distribution becomes unstable and flows towards one of the classical FPs $P(G) = \delta(G)$ or $P(G) = \delta(G - 1)$. We note that the FP distribution can be stabilized by forcing $P_n(G)$ to be symmetric with respect to $G = 0.5$ in the course of the RG procedure.

Fig. 2 illustrates the RG evolution of $P(G)$ and $Q(z)$. In order to reduce statistical fluctuations we average the FP distributions obtained from different $P_0(G)$. The FP distribution $P_c(G)$ exhibits a flat minimum around $G = 0.5$ and sharp peaks close to $G = 0$ and $G = 1$. It is symmetric with respect to $G \approx 0.5$ with $\langle G \rangle = 0.498 \pm 0.004$, where the error is the standard error of the mean of the obtained FP distribution. The FP distribution $Q_c(z)$ is close to Gaussian.

We now turn to the critical exponent ν . As a result of a general instability of the FP distribution, an initial shift of $Q_c(z)$ by a value z_0 results in the further drift of the maximum position, $z_{\max, n}$, away from $z = 0$ after each RG step. As expected, $z_{\max, n}$ depends linearly on z_0 . This dependence is shown in Fig. 3 (inset) for different n from 1 to 8. The critical exponent is then calculated from the slope according to Eq. (2). Fig. 3 illustrates how the critical exponent converges with n to the value 2.39 ± 0.01 . The error corresponds to a confidence interval of 95% as obtained from the fit to a linear behavior.

Due to the high accuracy of our calculation of $P_c(G)$, we were able to reliably determine many central moments

$\langle(G - \langle G \rangle)^m\rangle$ of the FP distribution $P_c(G)$. These moments are plotted in Fig. 4.

D. Comparison with previous simulations

By dividing the CC network into units, the RG approach completely disregards the interference of the wave function amplitudes between different units at each RG step. For this reason it is not clear to what extent this approach captures the main features and reproduces the quantitative predictions at the QH transition. Therefore, a comparison of the RG results with the results of direct simulations of the CC model is crucial. These direct simulations are usually carried out by employing either the quasi-1D version [63] or the 2D version [64] of the transfer-matrix method. The results of application of the version [63] to the CC model are reported in Refs. [26,27]. In Refs. [65–67] the version [64] was utilized. For the critical exponent the values $\nu = 2.5 \pm 0.5$ [26] and later $\nu = 2.4 \pm 0.2$ [27] were obtained. Note that our result is in excellent agreement with these values and is also consistent with the most precise $\nu = 2.35 \pm 0.03$ [2]. This already indicates a remarkable accuracy of the RG approach. In Refs. [65–67] the critical distribution $P_c(G)$ of the conductance was studied. $P_c(G)$ was found to be broad, which is in accordance with Fig. 2. However, a more detailed comparison is impossible, since the results of the simulations [65–67] do not obey the electron-hole symmetry condition $P_c(G) = P_c(1 - G)$. On the other hand, within the RG approach, the latter condition is satisfied automatically. Nevertheless, we can compare the moments of $P_c(G)$ to those calculated in Refs. [65,66]. They are presented in Fig. 4. In Ref. [66] only the standard deviation $(\langle G^2 \rangle - \langle G \rangle^2)^{1/2} \approx 0.3$ was computed. Our result is 0.316. In Ref. [65] the moments were fitted by two analytical functions which are also shown in Fig. 4. They agree with our calculations up to the 6-th moment. Here we point out that the moments obtained in Ref. [65] can hardly be distinguished from the moments of a uniform distribution. This reflects the fact that $P_c(G)$ is practically flat except for the peaks close to $G = 0$ and $G = 1$.

In Refs. [68,69] $P_c(G)$ was studied by methods which are not based on the CC model. Both works report a broad distribution $P_c(G)$. In Ref. [68] $P_c(G)$ was found to be almost flat. The major difference between Ref. [68] and Fig. 4 is the behavior of $P_c(G)$ near the points $G = 0$ and $G = 1$. Namely, $P(G)$ drops in Ref. [68] to zero at the ends, while Fig. 4 exhibits maxima. In Ref. [69] the behavior of $P_c(G)$ is qualitatively similar to Fig. 4 with maxima at $G = 0$ and $G = 1$. However, the statistics in Ref. [69] is rather poor, which again rules out the possibility of a more detailed comparison with our results.

Finally, we point out that our results agree completely with Refs. [70–72] where a similar RG treatment of the

CC model was carried out. Our numerical data have a higher resolution and show significantly less statistical noise. This is because we took advantage of faster computation by using the analytical solution of the RG Eq. (1) [55]. Note also, that in Refs. [70,72] the critical exponent ν was calculated using a procedure different from that described in Sec. II B. Nevertheless, the values of ν determined by both methods are close. We emphasize that a systematic improvement of the RG procedure, i.e., by inclusion of more than 5 SPs into the basic RG unit as reported in Refs. [70–72], leads to similar results. The critical distribution of the conductance was also studied experimentally [73,74] in mesoscopic QH samples. Although an almost uniform conductance distribution consistent with theoretical predictions was found in Ref. [73], further detailed analysis of the mesoscopic pattern [74] has revealed the crucial role of the charging effects, which were neglected in all theoretical studies.

We conclude that the test of the RG approach against other simulations proves that this approach provides a very accurate quantitative description of the QH transition. It can now be used to study the influence of long-ranged correlations.

III. MACROSCOPIC INHOMOGENEITIES

A. General considerations

A natural way to incorporate a quenched disorder into the CC model is to ascribe a certain random shift, z_Q , to each SP height and to assume that the shifts at different SP positions, \mathbf{r} and \mathbf{r}' , are correlated as

$$\langle z_Q(\mathbf{r})z_Q(\mathbf{r}') \rangle \propto |\mathbf{r} - \mathbf{r}'|^{-\alpha}, \quad (3)$$

with $\alpha > 0$. After that, the conventional transfer-matrix methods [63,64] could be employed for numerically precise determination of $\langle G \rangle$, the distribution $P_c(G)$, its moments, and most importantly, the critical exponent, ν . However, the transfer-matrix approach for a 2D sample is usually limited to fairly small sizes (e.g., up to 128 in Ref. [67]) due to the numerical complexity of the calculation. Therefore the spatial decay of the power-law correlation by, say, more than an order in magnitude is hard to investigate for small α . In principle the quasi-1D transfer-matrix method [26,63] can easily handle such decays at least in the longitudinal direction where typically a few million lattice sites are considered iteratively. A major drawback, however, is the numerical generation of power-law correlated randomness since no iterative algorithm is known [75,76]. This necessitates the complete storage of different samples of correlated SP height landscapes [77] and the advantage of the iterative transfer-matrix approach is lost. Furthermore, in order to deduce the critical exponent [27], one needs to perform finite-size scaling [63] with transverse sizes that should be large

enough to capture the main effect of the power-law disorder in the transverse direction, too. Consequently, even for a single transfer-matrix sample, the memory requirements add up to Gigabytes.

On the other hand, the RG approach is perfectly suited to study the role of the quenched disorder. Firstly, after each step of the RG procedure, the effective system size doubles. At the same time, the magnitude of the smooth potential, corresponding to the spatial scale r , falls off with r as $r^{-\alpha/2}$. As a result, the modification of the RG procedure due to the presence of the quenched disorder reduces to a rescaling of the disorder magnitude by a *constant* factor $2^{-\alpha/2}$ at each RG step. Secondly, the RG approach operates with the conductance distribution, $P_n(G)$, which carries information about *all* the realizations of the quenched disorder within a sample of a size 2^n . This is in contrast to the transfer-matrix approach [63,64], within which a small increase of the system size requires the averaging over the quenched disorder realizations to be conducted again.

In order to find out whether or not the critical behavior is affected by the quenched disorder, the following argument was put forward in Ref. [24]. In the absence of the quenched disorder, the correlation length, ξ_0 , for a given energy z_Q in the vicinity of the transition is proportional to $z_Q^{-\nu}$. Consider now a sample with an area $A = \xi_0^2$. The variance of the quenched disorder within the sample is given by

$$\begin{aligned} \Delta_0^2 &= \frac{1}{A^2} \langle \int_A d^2r z_Q(\mathbf{r}) \int_A d^2r' z_Q(\mathbf{r}') \rangle \\ &= \frac{1}{A^2} \int_A d^2r \int_A d^2r' \langle z_Q(\mathbf{r}) z_Q(\mathbf{r}') \rangle \\ &\propto \xi_0^{-2} \int_0^{\xi_0} dr r^{1-\alpha}, \end{aligned} \quad (4)$$

where the last relation follows from Eq. (3).

The critical behavior remains unaffected by the quenched disorder if the condition $\Delta_0^2/z_Q^2 \rightarrow 0$ as $z_Q \rightarrow 0$ is met. Using (4), the ratio Δ_0^2/z_Q^2 can be presented as

$$\frac{\Delta_0^2}{z_Q^2} \propto \begin{cases} z_Q^{2\nu-2}, & \alpha > 2 \\ z_Q^{2\nu-2} \ln(z_Q^{-\nu}), & \alpha = 2 \\ z_Q^{\alpha\nu-2}, & \alpha < 2 \end{cases} \quad (5)$$

We thus conclude that quenched disorder is irrelevant when

$$\begin{aligned} \nu > 1, & \quad \text{for } \alpha \geq 2 \quad \text{and} \\ \alpha\nu > 2, & \quad \text{for } \alpha < 2 \end{aligned} \quad (6)$$

The first condition corresponds to the original Harris criterion [78] for uncorrelated disorder, while the second condition is the extended Harris criterion [24]. It yields the critical value of the exponent α , i. e. $\alpha_c = 2/\nu$.

The above consideration suggests the following algorithm. For the homogeneous case all SPs constituting the new super-SP are assumed to be identical, which means that the distribution, of heights, $Q_n(z)$, for all of them is the same. For the correlated case these SPs are no longer identical, but rather their heights are randomly

shifted by the long-ranged potential. In order to incorporate this potential into the RG scheme, $Q_n(z_i)$ should be replaced by $Q_n(z_i - \Delta_i^{(n)})$ for each SP, i , where $\Delta_i^{(n)}$ is the random shift. Then the power-law correlation of the quenched disorder enters into the RG procedure through the distribution of $\Delta_i^{(n)}$. Namely, for each n the distribution is Gaussian with the width $\beta(2^n)^{-\alpha/2}$. For large enough n the critical behavior should not depend on the magnitude β , but on the power, α , only.

B. Numerical Results

Here we report the results of the application of the algorithm outlined in the previous section. Firstly, we find that for all values of $\alpha > 0$ in the correlator (3) the FP distribution is identical to the uncorrelated case within the accuracy of our calculation. In particular, $\langle G \rangle = 0.498$ is unchanged. However, the convergence to the FP is numerically less stable than for uncorrelated disorder due to the correlation-induced broadening of $Q_n(z)$ during each iteration step. In order to compute the critical exponent $\nu(\alpha)$ we start the RG procedure from $Q_0(z - z_0)$, as in the uncorrelated case, but, in addition, we incorporate the random shifts caused by the quenched disorder in generating the distribution of z at each RG step. The results shown in Fig. 5 illustrate that for increasing long-ranged character of the correlation (decreasing α) the convergence to a limiting value of ν slows down drastically. Even after 8 RG steps (i.e. magnification of the system size by a factor of 256), the value of ν with long-ranged correlations still differs appreciably from $\nu = 2.39$ obtained for the uncorrelated case. The RG procedure becomes unstable after 8 iterations, i.e., $z_{\max,9}$ can no longer be obtained reliably from $Q_9(z)$. Unfortunately, for small α the convergence is too slow to yield the limiting value of ν after 8 steps only. Therefore, we are unable to unambiguously determine whether sufficiently long-ranged correlations result in α -dependent critical exponent $\nu(\alpha)$, or the value of ν eventually approaches the uncorrelated value of 2.39. Nevertheless, the results in Fig. 5 indicate that the effective critical exponent exhibits sensitivity to the long-ranged correlations even after a large magnification by 256×256 . Therefore, in realistic samples of finite sizes, macroscopic inhomogeneities are able to affect the results of scaling studies. Note further that as shown in the inset of Fig. 5 there is no simple scaling of ν values when plotted as function of an renormalized system size $2^{\alpha n/2}$. We emphasize that $\nu(\alpha)$ obtained after 8 RG steps always *exceeds* the uncorrelated value. Thus, our results indicate that macroscopic inhomogeneities must lead to smaller values of $\kappa \propto 1/\nu$. Experimentally, the value of κ smaller than 0.42 was reported in a number of early (see, e.g., [7] and references therein) as well as recent [79] works. This fact was accounted for by different reasons (such as temperature dependence of the phase breaking

time, incomplete spin resolution, valley degeneracy in Si-based MOSFETs, and inhomogeneity of the carrier concentration in GaAs-based structures with a wide spacer). Briefly, the spread of the κ -values was attributed to the fact that the temperatures were not low enough to assess the truly critical regime. The possibility of having $\kappa < 0.4$ due the correlations-induced dependence of the effective ν on the phase-breaking length or, ultimately, on the sample size, as in Fig. 5, was never considered before.

Fig. 6 shows the values of ν obtained after the 8-th RG step as a function of the correlation exponent α for different dimensionless strengths, β , of the quenched disorder. It is seen that in the domain of α , where the values of ν differ noticeably from $\nu = 2.39$, their dependence on β is strong. According to the extended Harris criterion, $\nu(\alpha)$ is expected to exhibit a cusp at the β -independent value $\alpha = \alpha_c = 2/2.39 \approx 0.84$. Our results in Fig. 6 do not reveal such a cusp. A possible origin of this disagreement is a profound difference between the classical and quantum percolation problems. This difference is discussed in the next Section.

IV. CONCLUSION

In the classical limit, the motion of an electron in a strong magnetic field and a smooth potential reduces to the drift of the Larmour circle along the equipotential lines. Correspondingly, the description of the delocalization transition reduces to the classical percolation problem. As it was mentioned above, for classical percolation the quenched disorder is expected to cause a crossover in the exponent, ν_c , describing the size of a critical equipotential from $\nu_c = 4/3$ to $\nu_c = 2/\alpha$ for $\alpha < 3/2$. This prediction [25] was made on the basis of Eq. (4). It was later confirmed by numerical simulations [75], although the values of ν_c inferred from numerics for $\alpha > 1$ were consistently lower than $2/\alpha$.

The classical version of the delocalization transition is instructive, since it allows to trace how the critical equipotentials grow in size upon approaching the percolation threshold, and how the quenched disorder affects this growth. Roughly speaking, in the absence of the long-ranged correlations, the growth of the equipotential size is due to the attachment of smaller equipotentials to the critical ones. As a result, the shape of a critical equipotential is dendrite-like. As the threshold is approached, different critical equipotentials get connected through the narrow “arms” of the dendrite. Long-ranged correlations change this scenario drastically. As it could be expected intuitively, and follows from the simulations [76], critical equipotentials become more compact due to correlations. In fact, for $\alpha < 0.25$, the “arms” play no role [75], i.e., the morphology of a critical equipotential becomes identical to its “backbone”. As a result, the formation of the infinite equipotential at the threshold

occurs through a sequence of “broad” merges of compact critical equipotentials. The correlation-induced enhancement of ν_c indicates that due to these merges the size of the critical equipotential in the close vicinity of the threshold grows faster than in the uncorrelated case.

Since our simulations also demonstrate the enhancement of the critical exponent due to the correlations, the main result of the present paper can be formulated as: quenched disorder affects classical and quantum percolation in a similar fashion.

Note however, that there is a crucial distinction between the classical case and the quantum regime of the electron motion considered in the present paper. Indeed, within the classical picture, correlated disorder implies that the motion of the guiding centers of the Larmour orbits in two neighboring regions is completely identical. In our study, we have incorporated the correlation of *heights* of the saddle points into the RG scheme. At the same time we have assumed that the *Aharonov-Bohm phases* acquired by an electron upon traversing the neighboring loops are completely *uncorrelated*. This assumption implies that, in addition to the long-ranged potential, a certain short-ranged disorder causing the spread in the perimeters of neighboring loops of the order of the magnetic length is present in the sample. Rigorous generalization of the classical percolation to the quantum case would require the phases Φ_i to be correlated together with the SP heights z_i . This is probably the reason why we do not observe a cusp in the $\nu(\alpha)$ dependence at $\alpha \approx 0.84$ as might be expected from the extended Harris criterion. For the same reason our results for $\nu(\alpha)$ are sensitive to the value of parameter β which parameterizes the magnitude of the correlated potential. However, our calculation is more relevant to the experimental situation.

Eight RG steps allow us to trace the evolution of the wave functions from the *microscopic* scales (of the order of the magnetic length) to the *macroscopic* scales (of the order of $5\mu m$) which are comparable to the sizes of the samples used in the experimental studies of scaling (see e.g. Refs. [6,7]) and much bigger than the samples [73,74] used for the studies of mesoscopic fluctuations.

In conclusion, it was argued for a long time that the enhanced value of the critical exponent ν extracted from the narrowing of the transition region with temperature has its origin in the long-ranged disorder present in GaAs-based samples. The present work is the first attempt to quantify this argument. We indeed find that the random potential with a power-law correlator leads to the values of ν exceeding $\nu \approx 2.35$ which is firmly established for short-ranged disorder. Another *qualitative* conclusion of our study is that the spatial scale at which the exponent ν assumes its “infinite-sample” value is much larger in the presence of the quenched disorder than in the uncorrelated case. In fact this scale can be of the order of microns. This conclusion can also have serious experimental implications. Namely, even if the sample size is much bigger than this characteristic scale, this scale can

still exceed the phase-breaking length, which would mask the true critical behavior at the QH transition.

Our numerical results demonstrate that when the critical exponent depends weakly on the sample size (large n in Fig. 5), the “saturated” value of ν depends crucially on the “strength”, β , of the quenched disorder. Thus, it is important to relate this strength to the observable quantities. We can roughly estimate β assuming that the microscopic spatial scale (lattice constant) is the magnetic length, l , while the microscopic energy scale (the SP height) is the width of the Landau level. Denote with γ a typical fluctuation of the filling factor within a region with the size L . Then the estimate for β is $\beta \sim \gamma(L/l)^{\alpha/2}$. Naturally, for a given γ , the larger values of α correspond to the “stronger” quenched disorder parameter β .

Note finally, that throughout the paper we have considered the localization of a single electron. The role of electron-electron interactions in the scaling of the integer QH effect was recently addressed in Refs. [80,81].

ACKNOWLEDGMENTS

We thank F. Evers, F. Hohls, R. Klesse, G. Landwehr, A. Mirlin, and A. Zee for stimulating discussions. This work was supported by the NSF-DAAD collaborative research grant INT-0003710. PC, RAR, and MS also gratefully acknowledge the support of DFG within the Schwerpunktprogramm “Quanten-Hall-Systeme” and SFB 393.

-
- [1] B. Huckestein, *Rev. Mod. Phys.* **67**, 357 (1995).
[2] B. Huckestein and B. Kramer, *Phys. Rev. Lett.* **64**, 1437 (1990); B. Huckestein, *Europhys. Lett.* **20**, 451 (1992).
[3] H. P. Wei, D. C. Tsui, and A. M. M. Pruisken, *Phys. Rev. B* **33**, 1488 (1985).
[4] H. P. Wei, D. C. Tsui, M. A. Paalanen, and A. M. M. Pruisken, *Phys. Rev. Lett.* **61**, 1294 (1988).
[5] S. Koch, R. J. Haug, K. v. Klitzing, and K. Ploog, *Phys. Rev. B* **43**, 6828 (1991).
[6] S. Koch, R. J. Haug, K. v. Klitzing, and K. Ploog, *Phys. Rev. Lett.* **67**, 883 (1991).
[7] S. Koch, R. J. Haug, K. v. Klitzing, and K. Ploog, *Phys. Rev. B* **46**, 1596 (1992).
[8] H. P. Wei, S. Y. Lin, D. C. Tsui, and A. M. M. Pruisken, *Phys. Rev. B* **45**, 3926 (1992).
[9] S. W. Hwang, H. P. Wei, L. W. Engel, D. C. Tsui, and A. M. M. Pruisken, *Phys. Rev. B* **48**, 11416 (1993).
[10] The importance of the character of the disorder (short-ranged versus long-ranged) for the true scaling behavior of the components of the conductivity tensor was recently also emphasized in P. T. Coleridge, *Phys. Rev. B* **60**, 4493 (1999); P. T. Coleridge and P. Zawadzki, *Solid State Commun.*, **112**, 241 (1999).
[11] D. Shahar, M. Hilke, C. C. Li, D. C. Tsui, S. L. Sondhi, and M. Razeghi, *Solid State Commun.* **107**, 19 (1998).
[12] N. Q. Balaban, U. Meirav, and I. Bar-Joseph, *Phys. Rev. Lett.* **81**, 4967 (1998).
[13] L. W. Engel, D. Shahar, C. Kurdak, and D. C. Tsui, *Phys. Rev. Lett.* **71**, 2638 (1993).
[14] E. Shimshoni, A. Auerbach, and A. Kapitulnik, *Phys. Rev. Lett.* **80**, 3352 (1998).
[15] E. Shimshoni, *Phys. Rev. B* **60**, 10691 (1999).
[16] S. H. Simon and B. I. Halperin, *Phys. Rev. Lett.* **73**, 3278 (1994).
[17] I. M. Ruzin, N. R. Cooper, and B. I. Halperin, *Phys. Rev. B* **53**, 1558 (1996).
[18] N. R. Cooper, B. I. Halperin, C.-K. Hu, and I. M. Ruzin, *Phys. Rev. B* **55**, 4551 (1997).
[19] R. T. F. van Schaijk, A. de Visser, S. M. Olsthoorn, H. P. Wei, and A. M. M. Pruisken, *Phys. Rev. Lett.* **84**, 1567 (2000).
[20] F. Kuchar, R. Meisels, K. Dybko, and B. Kramer, *Europhys. Lett.* **49**, 480 (2000).
[21] F. Hohls, U. Zeitler, R. J. Haug, and K. Pierz, *ArXiv: cond-mat/0010417*.
[22] F. Hohls, U. Zeitler, and R. J. Haug, *ArXiv: cond-mat/0011009*.
[23] We emphasize that sometimes the term “long-ranged disorder” is also used for a disorder that has a finite correlation radius but which is larger than the magnetic length, see, e.g., F. Evers, A. D. Mirlin, D. G. Polyakov, and P. Wölfle, *Phys. Rev. B* **60**, 8951 (1999). This is different from the present situation.
[24] A. Weinrib and B. I. Halperin, *Phys. Rev. B* **27**, 413 (1983).
[25] A. Weinrib, *Phys. Rev. B* **29**, 387 (1984).
[26] J. T. Chalker and P. D. Coddington, *J. Phys. C* **21**, 2665 (1988).
[27] D.-H. Lee, Z. Wang, and S. Kivelson, *Phys. Rev. Lett.* **70**, 4130 (1993).
[28] D. K. K. Lee and J. T. Chalker, *Phys. Rev. Lett.* **72**, 1510 (1994).
[29] Z. Wang, D.-H. Lee, and X.-G. Wen, *Phys. Rev. Lett.* **72**, 2454 (1994).
[30] D. K. K. Lee, J. T. Chalker, and D. Y. K. Ko, *Phys. Rev. B* **50**, 5272 (1994).
[31] V. Kagalovsky, B. Horovitz, and Y. Avishai, *Phys. Rev. B* **52**, R17044 (1995).
[32] V. Kagalovsky, B. Horovitz, and Y. Avishai, *Phys. Rev. B* **55**, 7761 (1997).
[33] R. Klesse and M. Metzler, *Europhys. Lett.* **32**, 229 (1995).
[34] R. Klesse and M. Metzler, *Phys. Rev. Lett.* **79**, 721 (1997).
[35] I. Ruzin and S. Feng, *Phys. Rev. Lett.* **74**, 154 (1995).
[36] M. Metzler, *J. Phys. Soc. Japan* **67**, 4006 (1998).
[37] M. Janssen, M. Metzler, and M. R. Zirnbauer, *Phys. Rev. B* **59**, 15836 (1999).
[38] R. Klesse and M. R. Zirnbauer, *ArXiv: cond-mat/0010005*.
[39] B. Shapiro, *Phys. Rev. Lett.* **48**, 823 (1982).

[40] P. Freche, M. Janssen, and R. Merkt, in *Proceedings of the Ninth International Conference on Recent progress in Many Body Theories*, edited by D. Neilson (World Scientific, Singapore, 1998).

[41] R. Merkt, M. Janssen, and B. Huckestein, *Phys. Rev. B* **58**, 4394 (1998).

[42] M. Janssen, *Phys. Rep.* **295**, 1 (1998).

[43] P. Freche, M. Janssen, and R. Merkt, *Phys. Rev. Lett.* **82**, 149 (1999).

[44] V. Kagalovsky, B. Horovitz, Y. Avishai, and J. T. Chalker, *Phys. Rev. Lett.* **82**, 3516 (1999).

[45] J. T. Chalker, N. Read, V. Kagalovsky, B. Horovitz, Y. Avishai, and A. W. W. Ludwig, ArXiv: cond-mat/0009463.

[46] D.-H. Lee, *Phys. Rev. B* **50**, 10788 (1994).

[47] M. R. Zirnbauer, *Ann. Phys. (Leipzig)* **3**, 513 (1994).

[48] M. R. Zirnbauer, *J. Math. Phys.* **38**, 2007 (1997).

[49] I. A. Gruzberg, N. Read, and S. Sachdev, *Phys. Rev. B* **55**, 10593 (1997).

[50] A. W. W. Ludwig, M. P. A. Fisher, R. Shankar, and G. Grinstein, *Phys. Rev. B* **50**, 7526 (1994).

[51] Y. B. Kim, *Phys. Rev. B* **53**, 16420 (1996).

[52] C.-M. Ho and J. T. Chalker, *Phys. Rev. B* **54**, 8708 (1996).

[53] J. Kondev and J. B. Marston, ArXiv: cond-mat/9612223.

[54] J. B. Marston and S. Tsai, *Phys. Rev. Lett.* **82**, 4906 (1999).

[55] A. G. Galstyan and M. E. Raikh, *Phys. Rev. B* **56**, 1422 (1997).

[56] D. P. Arovas, M. Janssen, and B. Shapiro, *Phys. Rev. B* **56**, 4751 (1997).

[57] A very different reformulation of the problem of electron motion in a strong magnetic field in a random potential, which should be suitable for RG analysis, was recently proposed in J. Sinova, V. Meden, and S. M. Girvin, *Phys. Rev. B* **62**, 2008 (2000) and elaborated further in J. E. Moore, A. Zee, and J. Sinova, ArXiv: cond-mat/0012341; S. Boldyrev and V. Gurarie, ArXiv: cond-mat/0009203; V. Gurarie and A. Zee, ArXiv: cond-mat/0008163.

[58] U. Zülicke and E. Shimshoni, ArXiv: cond-mat/0101443.

[59] D. Stauffer and A. Aharony, *Introduction to Percolation Theory* (Taylor and Francis, London, 1992).

[60] P. J. Reynolds, W. Klein, and H. E. Stanley, *J. Phys. C* **10**, L167 (1977).

[61] J. Bernasconi, *Phys. Rev. B* **18**, 2185 (1978).

[62] W. H. Press, B. P. Flannery, S. A. Teukolsky, and W. T. Vetterling, *Numerical Recipes in FORTRAN*, 2nd ed. (Cambridge University Press, Cambridge, 1992).

[63] A. MacKinnon and B. Kramer, *Phys. Rev. Lett.* **47**, 1546 (1981).

[64] D. S. Fisher and P. A. Lee, *Phys. Rev. B* **23**, 6851 (1981).

[65] Z. Wang, B. Jovanovic, and D.-H. Lee, *Phys. Rev. Lett.* **77**, 4426 (1996).

[66] S. Cho and M. P. A. Fisher, *Phys. Rev. B* **55**, 1637 (1997).

[67] B. Jovanovic and Z. Wang, *Phys. Rev. Lett.* **81**, 2767 (1998).

[68] X. Wang, Q. Li, and C. M. Soukoulis, *Phys. Rev. B* **58**, 3576 (1998).

[69] Y. Avishai, Y. Band, and D. Brown, *Phys. Rev. B* **60**, 8992 (1999).

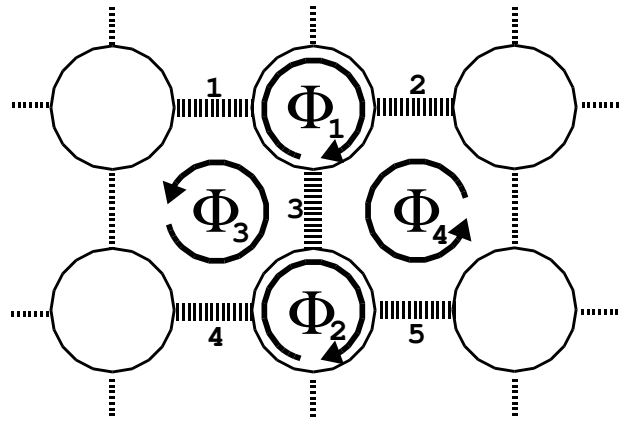


FIG. 1. Network of SPs (dashed lines) and equipotential lines (circles) on a square lattice. The RG unit used for Eq. (1) combines 5 SPs (numbered thick dashed lines) — in analogy with classical 2D bond percolation RG [60,61] — into a super-SP. Φ_1, \dots, Φ_4 are the phases acquired by an electron drifting along the contours indicated by the arrows.

[70] A. Weymer and M. Janssen, *Ann. Phys. (Leipzig)* **7**, 159 (1998).

[71] M. Janssen, R. Merkt, and A. Weymer, *Ann. Phys. (Leipzig)* **7**, 353 (1998).

[72] M. Janssen, R. Merkt, J. Meyer, and A. Weymer, *Physica B* **256–258**, 65 (1998).

[73] D. H. Cobden and E. Kogan, *Phys. Rev. B* **54**, R17316 (1996).

[74] D. H. Cobden, C. H. W. Barnes, and C. J. B. Ford, *Phys. Rev. Lett.* **82**, 4695 (1999).

[75] S. Prakash, S. Havlin, S. Schwartz, and H. E. Stanley, *Phys. Rev. A* **46**, R1724 (1992).

[76] H. Makse, S. Havlin, M. Schwartz, and H. E. Stanley, *Phys. Rev. E* **53**, 5445 (1996).

[77] S. Russ, J. W. Kantelhardt, A. Bunde, S. Havlin, and I. Webman, *Physica A* **266**, 492 (1999).

[78] A. B. Harris, *J. Phys. C* **7**, 1671 (1974).

[79] G. Landwehr, private communication, (2000); X.C. Zhang, A. Pfeuffer-Jeschke, K. Ortner, V. Hock, H. Buhmann, C. R. Becker, and G. Landwehr, *Zero field spin splitting in n-type modulation doped HgTe quantum wells with an inverted band structure*, preprint, (2001).

[80] B. Huckestein and M. Backhaus, *Phys. Rev. Lett.* **82**, 5100 (1999).

[81] Z. Wang, M. P. A. Fisher, M. Girvin, and J. T. Chalker, *Phys. Rev. B* **61**, 8326 (2000).

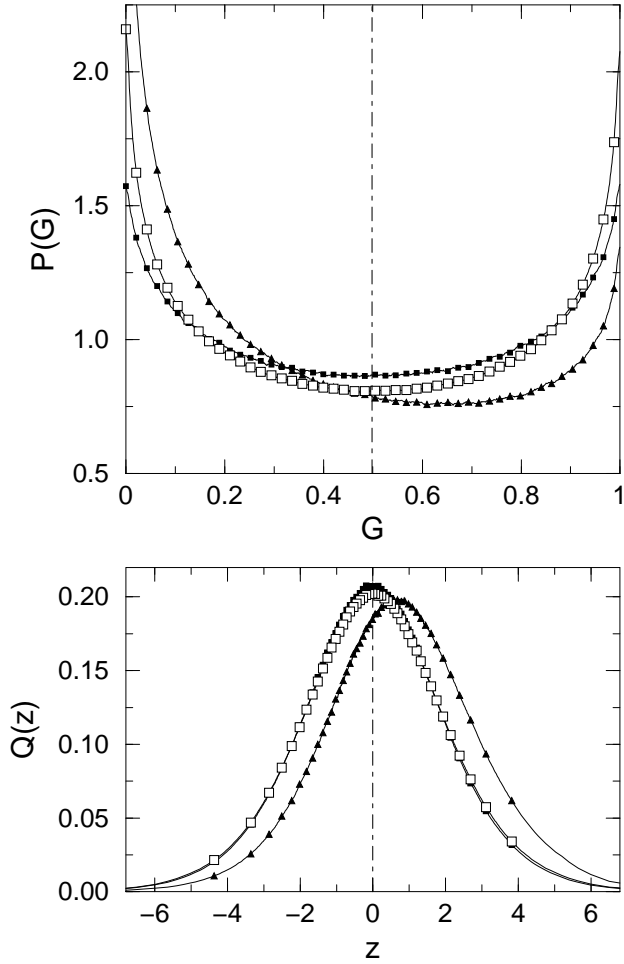


FIG. 2. Top: $P(G)$ (thin lines) as function of conductance G at a QH plateau-to-plateau transition. Symbols mark every 20-th data point for the initial distribution (\blacksquare), the FP (\square) and the distribution for RG step $n = 16$ (\blacktriangle). The vertical dashed line indicates the average of the FP distribution. Bottom: Corresponding plots for the distribution $Q(z)$ of SP heights.

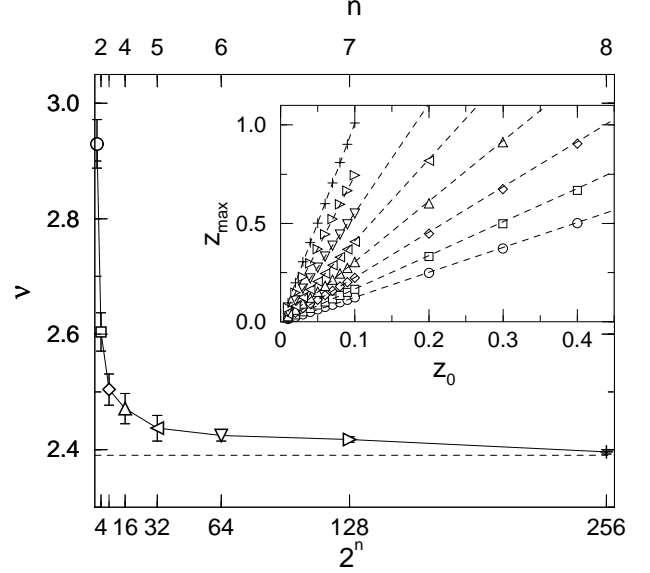


FIG. 3. Critical exponent ν obtained by the QH-RG approach as function of effective linear system size $L = 2^n$ for RG step n . The error bars correspond to the error of linear fits to the data. The dashed line shows $\nu = 2.39$. Inset: ν is determined by the dependence of the maximum $z_{\max, n}$ of $Q_n(z)$ on a small initial shift z_0 . Dashed lines indicate the linear fits.

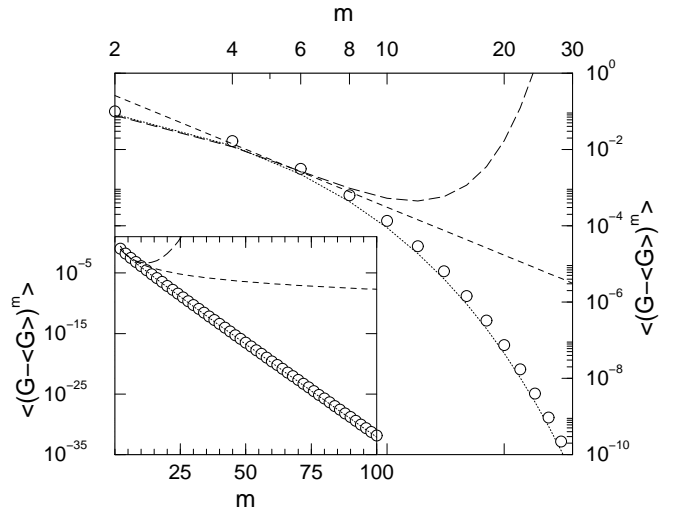


FIG. 4. Moments $\langle (G - \langle G \rangle)^m \rangle$ of the FP distribution $P_c(G)$ (\circ). Dashed lines are results of Ref. [65]. The dotted line corresponds to the moments of a constant distribution. Inset: Higher moments of $P_c(G)$ following an exponential behavior. The agreement of data and fit demonstrates the quality of the fit result.

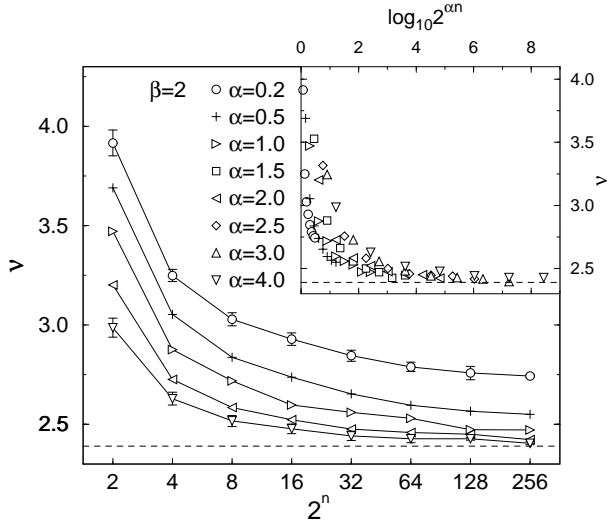


FIG. 5. Critical exponent ν obtained by QH-RG as function of RG scale 2^n for $\beta = 2$ and different correlation exponents α . The dashed line indicates $\nu = 2.39$, which is the value that we obtain for uncorrelated disorder. For clarity, we show the errors only for $\alpha = 0.2$ and 4. Inset: ν versus $2^{\alpha n/2}$ does not scale for, e.g., $\beta = 2$.

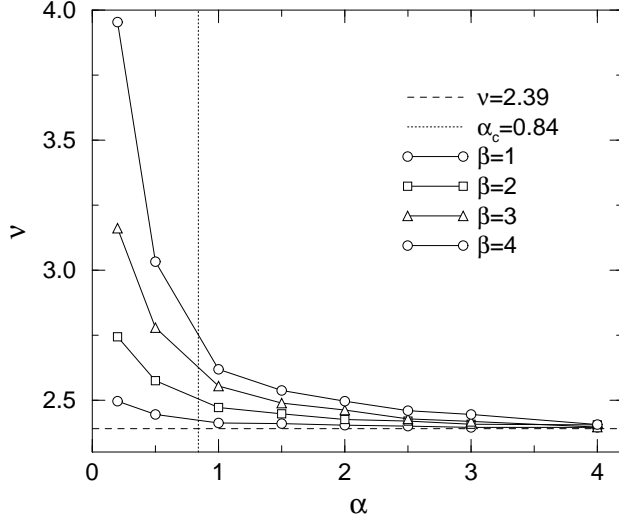


FIG. 6. Dependence of the critical exponent ν on correlation exponent α for different $\beta = 1, 2, 3$, and 4 as obtained after 8 QH-RG iterations. The dotted line indicates $\alpha_c = 0.84$ following from the extended Harris criterion [24] for classical percolation.